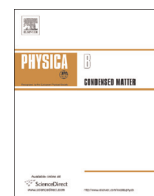




ELSEVIER

Contents lists available at ScienceDirect

Physica B

journal homepage: www.elsevier.com/locate/physb

Electron distribution in polar heterojunctions within a realistic model



Nguyen Thanh Tien ^{a,*}, Dinh Nhu Thao ^b, Pham Thi Bich Thao ^a, Doan Nhat Quang ^c

^a College of Natural Science, Can Tho University, 3-2 Road, Can Tho City, Vietnam

^b Center for Theoretical and Computational Physics, College of Education, Hue University, 34 Le Loi Street, Hue City, Vietnam

^c Institute of Physics, Vietnamese Academy of Science and Technology, 10 Dao Tan Street, Hanoi, Vietnam

ARTICLE INFO

Article history:

Received 16 January 2015

Received in revised form

17 July 2015

Accepted 22 September 2015

Available online 25 September 2015

Keywords:

Hetero-junction

Polar semiconductor

Electron distribution

Interface polarization charge

Finite potential barrier

Modulation doping

ABSTRACT

We present a theoretical study of the electron distribution, i.e., two-dimensional electron gas (2DEG) in polar heterojunctions (HJs) within a realistic model. The 2DEG is confined along the growth direction by a triangular quantum well with a finite potential barrier and a bent band figured by all confining sources. Therein, interface polarization charges take a double role: they induce a confining potential and, furthermore, they can make some change in other confinements, e.g., in the Hartree potential from ionized impurities and 2DEG. Confinement by positive interface polarization charges is necessary for the ground state of 2DEG existing at a high sheet density. The 2DEG bulk density is found to be increased in the barrier, so that the scattering occurring in this layer (from interface polarization charges and alloy disorder) becomes paramount in a polar modulation-doped HJ.

© 2015 Elsevier B.V. All rights reserved.

1. Introduction

Recently, electronic transport and intersubband optical transition in polar heterostructures (HSs), such as gallium nitride (GaN) (or zinc oxide (ZnO)), and their compounds have been intensively investigated [1,2]. These properties are characteristic of the quality and performance of electronic and optical devices [3]. The quoted semiconductors possess unique features that make them important to fabricate electronic and optical devices in view of their promising potential for high-voltage, high-power, and high-temperature microwave applications.

The electronic transport in a HS is characterized by a high mobility of two-dimensional electron gas (2DEG) in the sample, and its optical absorption by a narrow spectral linewidth. Both properties in question are determined by various scattering processes taking place with 2DEG. The effect of a scattering process in the lateral plane is determined by its mechanism, but this also depends on the electron distribution along the growth direction (quantization direction). Thus, the effect of an electron scattering process in the lateral plane depends on the envelope function, i.e., on confinement sources.

As is well known [1,2], polarization is an important property of a nitride and oxide-based HS. The HS possesses a very high (areal)

density of polarization charges bound on the interface ($\sigma \sim 10^{13} \text{ cm}^{-2}$). For formation of 2DEG in a polar HS, interface polarization charges take a double role: they are a source to supply carriers (electrons) into the sample, but they also are a source to confine the carriers along the growth direction. It is worth noting that for formation of 2DEG in a modulation-doped HS, ionized impurities take such a double role as well [3,4].

Therefore, the aim of this paper is to present a theoretical study of the electron distribution (2DEG) in a polar modulation-doped HS, where the above double role of both interface polarization charges and ionized impurities is reasonably taken into account. Especially, we want to compare the role of the interface polarization charges and the ionized impurities which has not been done so far.

For simple illustration, we deal with a two-layer HS, i.e., single heterojunction (HJ) based on GaN. In Section 2, the 2DEG in a HJ is assumed to occupy the ground subband. The corresponding electron state is approximately described by a variational wave function in a triangular quantum well (QW). Within this realistic model, the QW has a finite potential barrier and a bent band.

In Section 3, parameters figuring the variational wave function are determined for a polar modulation-doped HJ by all confining potentials, especially from interface polarization charges and ionized impurities. Numerical results illustrating the electron distribution in HJ are also presented in Section 3. Lastly, a summary is given in Section 4.

* Corresponding author.

E-mail address: thanhtientu@gmail.com (N.T. Tien).

2. Theory

2.1. Variational wave function for HJ of finite potential barrier

We are now dealing with wurtzite III-nitride-based HJs, e.g., an AlGaIn/GaN sample, which is composed of an AlGaIn layer grown on a GaN layer. The system is featured with the z -axis along and opposite to the growth direction [0001], and $z=0$ being the interface plane between the GaN channel ($z > 0$) and the AlGaIn barrier ($z < 0$). It is assumed that the channel layer (large thickness) is relaxed, while the barrier one (small thickness) is under tensile strain and modulation-doped.

At low temperature, the 2DEG is assumed to primarily occupy the lowest subband. It was shown [4–6] that in the realistic model of triangular QWs with a finite potential barrier, the electron state may be well described by a Fang–Howard wave function modified by Ando [5]:

$$\zeta(z) = \begin{cases} A\kappa^{1/2} \exp(\kappa z/2) & \text{for } z < 0, \\ Bk^{1/2}(kz + c) \exp(-kz/2) & \text{for } z > 0. \end{cases} \quad (1)$$

Here, κ and k are half the wave numbers in the barrier and channel layers, respectively. A , B , and c are dimensionless parameters given in terms of k and κ through the boundary and normalization conditions, as follows [4,6]:

$$\begin{aligned} A\kappa^{1/2} &= Bk^{1/2}c, \\ A\kappa^{3/2}/2 &= Bk^{3/2}(1 - c/2), \\ A^2 + B^2(c^2 + 2c + 2) &= 1. \end{aligned} \quad (2)$$

The wave function of the lowest subband (its wave vectors k and κ) is to minimize the total energy per electron, which is fixed by the Hamiltonian

$$H = T + V_{\text{tot}}(z), \quad (3)$$

where T is the kinetic energy, and $V_{\text{tot}}(z)$ is the overall confining potential.

2.2. Confining potentials in a polar modulation-doped HS

Carrier confinement in a polar modulation-doped HS is determined by all confining sources located along the growth direction (z -axis): potential barrier, interface polarization charges, and Hartree potential induced by ionized impurities and 2DEG:

$$V_{\text{tot}}(z) = V_b(z) + V_\sigma(z) + V_H(z). \quad (4)$$

We are to specify the individual confining potentials in Eq. (4). First, for the potential barrier of a finite height V_0 located at the interface plane $z=0$, it holds

$$V_b(z) = V_0 \theta(-z), \quad (5)$$

with $\theta(z)$ as a unity step function. The potential barrier height is fixed by the conduction band offset between the AlGaIn and GaN layers: $V_0 = \Delta E_c(x)$, with x as the alloy (Al) content in the AlGaIn barrier.

It is well known [7–10] that due to piezoelectric and spontaneous polarizations in a nitride-based strained HS there exist positive polarization charges bound on the interface. These charges create a uniform normal electric field with the potential given by [11]

$$V_\sigma(z) = \frac{2\pi}{\epsilon_a} e\sigma|z|, \quad (6)$$

with σ as their total density. Here $\epsilon_a = (\epsilon_b + \epsilon_c)/2$ is the average value of the dielectric constants of the barrier (ϵ_b) and channel (ϵ_c).

Next, we calculate the Hartree potential induced by the ionized donors and 2DEG in the HS. This is determined according to Poisson's equation [6,12]

$$\frac{d^2}{dz^2} V_H(z) = \frac{4\pi e^2}{\epsilon_a} [N_I(z) - n(z)], \quad (7)$$

where $N_I(z)$ is the bulk density of donors along the growth direction, and $n(z)$ the one of electrons.

Hereafter, we are concerned with such samples that are modulation-doped in the barrier [13–15]:

$$N_I(z) = \begin{cases} N_I & \text{for } -z_d \leq z \leq -z_s, \\ 0 & \text{elsewhere,} \end{cases} \quad (8)$$

where $z_s = L_s$ and $z_d = L_s + L_d$, with L_s and L_d as the thicknesses of the spacer and doping layers, respectively.

The bulk density of electrons along the z -axis is determined by the envelope wave function in Eq. (1):

$$n(z) = n_s |\zeta(z)|^2, \quad (9)$$

with n_s as their sheet density.

We solve the Poisson equation for the Hartree potential $V_H(z)$ induced by the above distributions of the donors and 2DEG in combination with the boundary conditions at $z = \pm \infty$. For a non-polar HS, the subsystem composed of the donors and the 2DEG is neutral, so its electric field is vanishing at $z = \pm \infty$ [4,6,16]:

$$\partial V_H / \partial z (\pm \infty) = 0. \quad (10)$$

However, in a polar HS the 2DEG originates not only from donors, but also from polarization charges, the neutrality condition is not claimed on the donor-2DEG subsystem. Hence, the boundary condition at $z = -\infty$ must be different, given as follows [12]:

$$\partial V_H / \partial z (-\infty) = 0 \quad \text{and} \quad V_H(-\infty) = E_i, \quad (11)$$

with E_i as the binding energy of an ionized donor.

As a result, the Hartree potential may be represented in the form

$$V_H = V_I + V_s, \quad (12)$$

Here the first term is the potential due to remote donors, determined by the doping profile, viz., the donor sheet density ($n_I = N_I L_d$) and the thicknesses of the doping and spacer layers, given by

$$V_I(z) = E_i + \frac{4\pi e^2 n_I}{\epsilon_a} \begin{cases} 0 & \text{for } z < -z_d, \\ (z + z_d)^2 / 2L_d & \text{for } -z_d < z < -z_s, \\ z + (z_d + z_s)/2 & \text{elsewhere.} \end{cases} \quad (13)$$

The second term is the potential due to 2DEG, determined by the electron sheet density n_s and its z -axis distribution, i.e., the electron wave function, given by

$$V_s(z) = -\frac{4\pi e^2 n_s}{\epsilon_a} \begin{cases} f(z) & \text{for } z < 0, \\ g(z) + z + f(0) - g(0) & \text{for } z > 0. \end{cases} \quad (14)$$

The auxiliary functions in Eq. (14) are defined in terms of the variational parameters entering Eq. (1), as follows:

$$f(z) = \frac{A^2}{\kappa} e^{-\kappa z} \quad (15)$$

and

$$g(z) = \frac{B^2}{k} e^{-kz} [k^2 z^2 + 2k(c+2)z + c^2 + 4c + 6]. \quad (16)$$

2.3. Total energy per electron in the HJ lowest subband

We now turn to the total energy per electron when the 2DEG is occupying the ground subband. The expectation value of the Hamiltonian given by Eqs. (3) and (4) reads

$$E_0(k, \kappa) = \langle T \rangle + \langle V_b \rangle + \langle V_\sigma \rangle + \langle V_i \rangle + \langle V_s \rangle. \quad (17)$$

The total energy per electron is obtained by a modification of Eq. (17) in which the average 2DEG potential $\langle V_s \rangle$ is to be replaced with its half [4].

Upon employing the above-derived analytic expressions for the individual confining potentials, we may easily calculate their expectation values with the lowest-subband wave function from Eq. (1). The average energies figuring in Eq. (17) are supplied below.

For the kinetic energy, it holds

$$\langle T \rangle = -\frac{\hbar^2}{8m_z} [A^2\kappa^2 + B^2k^2(c^2 - 2c - 2)], \quad (18)$$

where m_z is the out of-plane effective mass of the GaN electron.

Next, for the potentials related to the barrier and the polarization charges bound on the interface, we have

$$\langle V_b \rangle = V_0 A^2, \quad (19)$$

and

$$\langle V_\sigma \rangle = \frac{2\pi e\sigma}{\epsilon_a} \left[\frac{A^2}{\kappa} + \frac{B^2}{k} (c^2 + 4c + 6) \right]. \quad (20)$$

For the potential due to ionized impurities, it holds

$$\begin{aligned} \langle V_i \rangle = E_i + \frac{4\pi e^2 n_i}{\epsilon_a} \left\{ \frac{d+s}{2\kappa} \right. \\ + \frac{A^2}{\kappa(d-s)} \left[\chi_2(d) - \chi_2(s) - d\chi_1(d) + s\chi_1(s) + \frac{d^2}{2} [\chi_0(d) - 1] \right. \\ \left. \left. - \frac{s^2}{2} [\chi_0(s) - 1] \right] + \frac{B^2}{k} (c^2 + 4c + 6) \right\}, \end{aligned} \quad (21)$$

with $s = \kappa L_s$ and $d = \kappa(L_d + L_s)$ as the dimensionless doping sizes. Here we introduced an auxiliary function

$$\chi_n(x) = 1 - e^{-x} \sum_{l=0}^n \frac{x^l}{l!}, \quad (22)$$

with $n = 0, 1, 2, \dots$ (an integer).

Lastly, the average 2DEG potential is given by

$$\begin{aligned} \langle V_s \rangle = -\frac{4\pi e^2 n_s}{\epsilon_a} \left[\frac{A^2}{\kappa} - \frac{A^4}{2\kappa} \right. \\ \left. + \frac{B^2}{k} (c^2 + 4c + 6) - \frac{B^4}{4k} (2c^4 + 12c^3 + 34c^2 + 50c + 33) \right]. \end{aligned} \quad (23)$$

3. Numerical results

In previous studies [15,17–20] of lateral 2DEG transport in HJs, the calculation was done within the ideal model of infinite-potential barrier, based on the standard Fang–Howard wave function [22]. This model simplified essentially the mathematics of the transport theory and was a good approximation for such scattering mechanisms that are insensitive to the near-interface wave function, as by phonons, ionized impurities, and charged dislocations.

In this paper we study the opposite case where the key scattering mechanisms are quite sensitive thereto [23,24]. Therefore, we examine the confinement effect within the realistic model of finite barrier, based on the modified Fang–Howard wave function [5]. As an example, we deal with the AlGaIn/GaN polar HJ of a finite

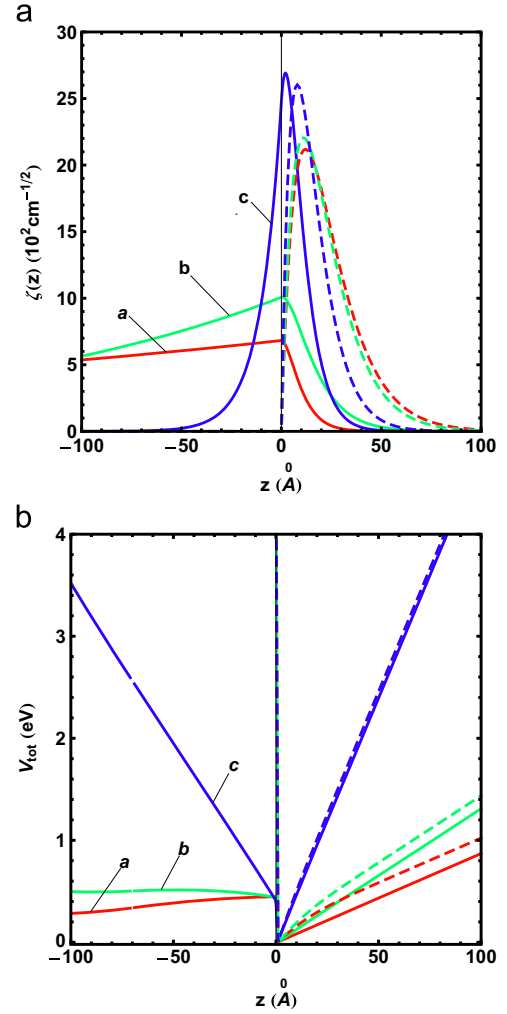


Fig. 1. Wave function $\zeta(z)$ (a) and confining potentials (b) in an AlGaIn/GaN HJ for a 2DEG density $n_s = 5 \times 10^{12} \text{ cm}^{-2}$, a modulation doping of donor bulk density $N_d = 5 \times 10^{18} \text{ cm}^{-3}$, doping thickness $L_d = 150 \text{ Å}$, spacer $L_s = 70 \text{ Å}$, and various polarization-charge densities $\sigma/e = 5 \times 10^{12}$, 10^{13} , and $5 \times 10^{13} \text{ cm}^{-2}$, labeled a, b, and c, respectively. Solid and dashed lines refer to the realistic model and the ideal model, respectively with the wave functions in (a) and the confining potentials in (b).

barrier being equal to the conduction band offset for $x=0.3$: $V_0 = 0.45 \text{ eV}$. Numerical results are similar for MgZnO/ZnO polar HJ. Hereafter, the dashed and solid lines refer to the infinite- and finite-barrier models, respectively. We are concerned with the dependence of the wave function on parameters of the supply and confinement sources, e.g., 2DEG, doping source, and polarization.

In Figs. 1 and 2, we display the standard (dashed lines) and modified (solid ones) Fang–Howard wave functions $\zeta(z)$ along the z -axis under modulation doping with a bulk density of donors $N_d = 5 \times 10^{18} \text{ cm}^{-3}$, and thickness for doping $L_d = 150 \text{ Å}$ and spacer $L_s = 70 \text{ Å}$.

In Fig. 1(a), these are plotted for a sheet density of 2DEG $n_s = 5 \times 10^{12} \text{ cm}^{-2}$ and various polarization-charge densities $\sigma/e = 5 \times 10^{12}$, 10^{13} , and $5 \times 10^{13} \text{ cm}^{-2}$, labeled a, b, and c, respectively. To demonstrate the bent band effect by the interface polarization charges, we display the total confining potential in Fig. 1(b).

In Fig. 2, these are plotted for a polarization-charge density $\sigma/e = 10^{13} \text{ cm}^{-2}$ and various sheet densities of 2DEG $n_s = 10^{12}$, 5×10^{12} , and 10^{13} cm^{-2} , labeled a, b, and c, respectively.

Next, we examine the doping effect in the AlGaIn/GaN HJ on the 2DEG distribution. The standard and modified Fang–Howard wave

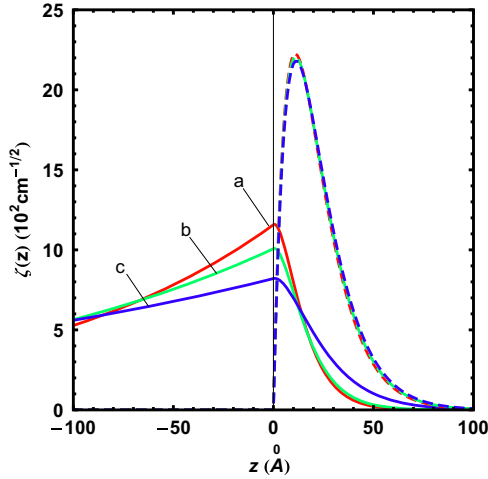


Fig. 2. Wave function $\zeta(z)$ in AlGaIn/GaN HS for an alloy (Al) content $x=0.3$, a modulation doping of $N_1 = 5 \times 10^{18} \text{ cm}^{-3}$, $L_d = 150 \text{ \AA}$, $L_s = 70 \text{ \AA}$, and various sheet 2DEG densities $n_s = 10^{12}$, 5×10^{12} , and 10^{13} cm^{-2} , labeled a, b, and c, respectively. The interpretation is the same as in Fig. 1.

functions $\zeta(z)$ are plotted in Fig. 3 for a polarization-charge density $\sigma/e = 10^{13} \text{ cm}^{-2}$ and a 2DEG sheet density $n_s = 5 \times 10^{12} \text{ cm}^{-2}$. The modulation doping is with a doping thickness $L_d = 150 \text{ \AA}$ and (a) a fixed spacer thickness $L_s = 70 \text{ \AA}$, and various donor densities $N_1 = 10^{18}$, 5×10^{18} , and 10^{19} cm^{-3} , labeled a, b, and c, respectively, and (b) a fixed donor density $N_1 = 5 \times 10^{18} \text{ cm}^{-3}$, and various spacer thicknesses $L_s = 0$, 70, and 150 \AA , labeled a, b, and c, respectively.

The numerical calculation reveals the fact that without interface polarization charges ($\sigma=0$) the ground state of 2DEG cannot exist at a high electron sheet density (e.g., $n_s = 10^{12} \text{ cm}^{-2}$).

From the lines thus obtained, we may draw the following conclusions.

As clearly seen from Figs. 1–3, the influence of confining sources on the electron wave function in the ideal (infinite barrier) and realistic (finite one) models is essentially different.

(i) Within the ideal model of infinite barrier (dashed lines), the peak of the wave function is raised when increasing the densities of interface polarization charges [16], ionized impurities, as well as decreasing the 2DEG [19]. But the wave functions are virtually unchanged when we change the spacer thickness.

(ii) This change is in sharp contrast to that in the realistic model of finite barrier (solid lines), where the wave function peak is lowered with the above variation of the parameters. Only the peak of the wave function is raised when increasing the densities of interface polarization charges [21].

The change of the wave function with variation of the confining parameters is explained as follows. For instance, for $\sigma > 0$, the polarization charges bound on the interface cause an attraction of electrons thereto. In the infinite-barrier model, the wave function cannot penetrate into the barrier, being squeezed, so that its peak is raised, its local slope at the interface plane, $\zeta'(z=0)$, is increased. On the contrary, in the finite-barrier model, the wave function can penetrate through the interface plane, so being shifted toward the barrier and its local value at the plane, $\zeta(0)$, is reduced.

As a result, combined roughness (CR) scattering, which is a combination of the effects from interface geometric roughness and polarization roughness, is found to be weakened [23]. Further, the value of the wave function at $z = -L_a$ near the interface is smaller, so alloy disorder (AD) scattering is also reduced [24].

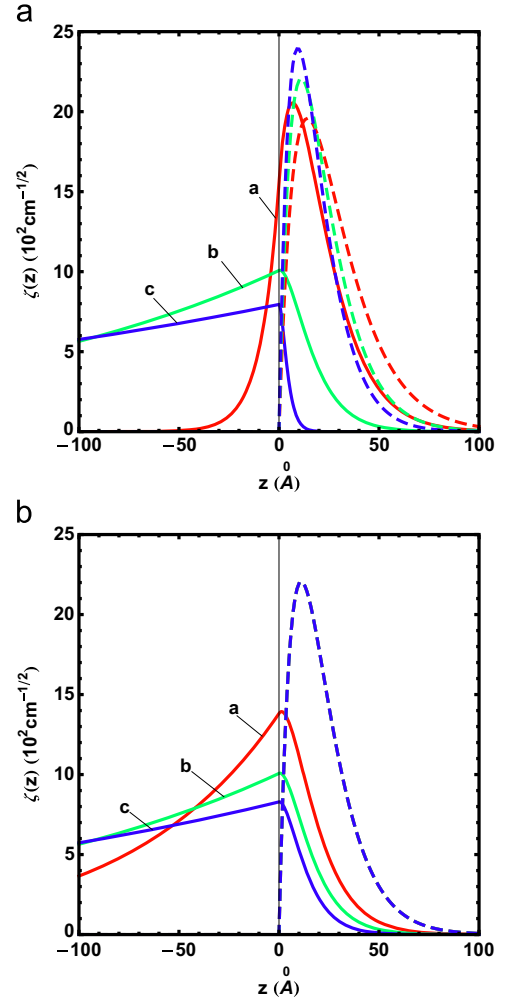


Fig. 3. Wave function $\zeta(z)$ in AlGaIn/GaN HS for an alloy (Al) content $x=0.3$, a 2DEG density $n_s = 5 \times 10^{12} \text{ cm}^{-2}$, and modulation doping with thickness $L_d = 150 \text{ \AA}$, and (a) a spacer thickness $L_s = 70 \text{ \AA}$ and various densities $N_1 = 10^{18}$, 5×10^{18} , and 10^{19} cm^{-3} , labeled a, b, and c, respectively, and (b) a density $N_1 = 5 \times 10^{18} \text{ cm}^{-3}$ and various spacer thicknesses $L_s = 0$, 70, and 150 \AA , labeled a, b, and c, respectively. The interpretation is the same as in Fig. 1. Note that, in the infinite barrier model, wave functions are virtually unchanged when the spacer thickness changes.

4. Summary

In this paper we study the electron distribution (2DEG) in polar HJs within the realistic model. The 2DEG is confined by triangular quantum well of a finite potential barrier and a bent band figured by all confinement sources. For a polar modulation-doped HJ, the confining effects from interface polarization charges and ionized impurities are properly taken into account.

We found out that the electron distribution in the realistic (finite barrier) and ideal (infinite one) models is changed in opposite directions in many cases when the carrier-supply and confinement sources are varying. Only the electron distribution is changed in the same trend when increasing the densities of interface polarization charges but they penetrate into the barrier when the height of barrier is finite.

Interface polarization charges are necessary to fabricate electronic devices with 2DEG in the ground state of high sheet density, so, of high electric conductivity.

The ideal model is applicable, as a good approximation, only to scatterings that are insensitive to the near-interface 2DEG distribution. For scatterings sensitive thereto, e.g., alloy disorder and roughness-related roughness, the realistic model must be applicable.

Acknowledgments

This work was supported by the Vietnamese National Foundation for Science and Technology Development (NAFOSTED 103.02-2012.04).

References

- [1] D. Jena, in: C. Wood, D. Jena (Eds.), *Polarization Effects in Semiconductors: From Ab Initio Theory to Device Applications*, Springer, New York, 2008, p. 161.
- [2] T. Yao, S.-K. Hong (Eds.), *Oxide and Nitride Semiconductors*, Springer, Berlin, Heidelberg, 2009.
- [3] T. Ando, A.B. Fowler, F. Stern, *Rev. Mod. Phys.* 54 (1982) 437.
- [4] G. Bastard, *Wave Mechanics Applied to Semiconductor Heterostructures*, Les Editions de Physique, Paris, 1988.
- [5] T. Ando, *J. Phys. Soc. Jpn.* 51 (1982) 3893;
T. Ando, *J. Phys. Soc. Jpn.* 51 (1982) 3900.
- [6] Y. Okuyama, N. Tokuda, *Phys. Rev. B* 40 (1989) 9744.
- [7] A. Bykhovski, G. Gelmont, M. Shur, *J. Appl. Phys.* 74 (1993) 6734.
- [8] F. Bernardini, V. Fiorentini, D. Vanderbilt, *Phys. Rev. B* 56 (1997) R10 024.
- [9] I.P. Smorchkova, C.R. Elsass, J.P. Ibbetson, R. Vetry, B. Heying, P. Fini, E. Haus, S. DenBaars, J.S. Spect, U.K. Mishra, *J. Appl. Phys.* 86 (1999) 4520.
- [10] O. Ambacher, B. Foutz, J. Smart, J.R. Shealy, N.G. Weimann, K. Chu, M. Murphy, A.J. Sierakowski, W.J. Shaff, L.F. Eastman, R. Dimitrov, A. Mitchell, M. Stutzmann, *J. Appl. Phys.* 87 (2000) 334.
- [11] D.N. Quang, N.H. Tung, N.T. Tien, *J. Appl. Phys.* 109 (2011) 113711.
- [12] R. Enderlein, N.J.M. Horing, *Fundamentals of Semiconductor Physics and Devices*, World Scientific, Singapore, 1997.
- [13] S. Keller, G. Parish, P.T. Fini, S. Heikman, C.-H. Chen, N. Zhang, S.P. DenBaars, U. K. Mishra, Y.-F. Wu, *J. Appl. Phys.* 86 (1999) 5850.
- [14] S. Arulkumaran, T. Egawa, H. Shikawa, T. Jimbo, *J. Vac. Sci. Technol. B* 21 (2003) 888.
- [15] M. Miyoshi, T. Egawa, H. Shikawa, *J. Vac. Sci. Technol. B* 23 (2005) 1527.
- [16] D.N. Quang, V.N. Tuoc, N.H. Tung, N.V. Minh, P.N. Phong, *Phys. Rev. B* 72 (2005) 245303.
- [17] D. Zanato, S. Gokden, N. Balkan, B.K. Ridley, W.J. Schaff, *Semicond. Sci. Technol.* 19 (2004) 427.
- [18] M.N. Gurusingham, S.K. Davidsson, T.G. Andersson, *Phys. Rev. B* 72 (2005) 045316.
- [19] J. Antoszewski, M. Gracey, J.M. Dell, L. Faraone, T.A. Fisher, G. Parish, Y.-F. Wu, U.K. Mishra, *J. Appl. Phys.* 87 (2000) 3900.
- [20] S. Gokden, *Phys. Stat. Sol. A* 200 (2003) 369.
- [21] V.M. Polyakov, V. Cimalla, V. Lebedev, K. Köhler, S. Müller, P. Waltereit, O. Ambacher, *Appl. Phys. Lett.* 97 (2010) 142112.
- [22] F.F. Fang, W.E. Howard, *Phys. Rev. Lett.* 16 (1966) 797.
- [23] D.N. Quang, L. Tuan, N.T. Tien, *Phys. Rev. B* 77 (2008) 125326.
- [24] D.N. Quang, N.T. Tien, D.N. Thao, P.T.B. Thao, *Phys. Rev. B* (2015), submitted for publication.